JSTEM

Electrostatic regulation of liquid-liquid phase separation of DNA-polypeptide system

Yu Zheng, Zhuliang Liu, Xuetong He, Jingxing Lu, Yi Shi, Guangcan Yang * and Yanwei Wang *

College of Mathmatics and Physics, Wenzhou University, China

wangyw@wzu.edu.cn ; yanggc@wzu.edu.cn

Abstract: Liquid-liquid phase separation (LLPS) of proteins and nucleic acids play an important role in the formation of membrane-less intracellular organelles and is related to some diseases due to abnormal protein aggregation. In the present study, we focus on the mechanism and regulation of LLPS of polylysine (PLL) and DNA solution. We found that the dominant interaction in PLL-DNA system is electronic force between them. Then we regulated its LLPS by adding ethanol and zwitterionic 6-Aminocaproic acid (6-A) which enhance and suppress electrostatic interaction between the macroions charged oppositely. The result showed when a fixed DNA concentration was kept in solution, LLPS occurred at a lower critical value of PLL concentration and disappeared at a higher critical concentration. The addition of ethanol shifted the range of LLPS upward, while 6-A shifted it downward. Specifically, for a fixed DNA concentration of 1 μg/μl, the critical PLL concentrations for LLPS were 0.4 μg/μl and 2 μg/μl, respectively. Upon addition of 20% ethanol, the critical PLL concentrations increased to 1 μg/μl and 4.5 μg/μl, respectively. On the other hand, the addition of 700 mM 6-A decreased the critical PLL concentrations to 0.35 μg/μl and 1 μg/μl, respectively. The results demonstrate that the adjustment of electrostatic interaction between DNA and counterions can effectively influence the LLPS of DNA.

Keywords: liquid-liquid phase separation, DNA, Polylysine, electrostatic interaction, 6-Aminocaproic acid, ethanol

1. Introduction

Liquid-liquid phase separation (LLPS) plays a crucial role in the formation of intracellular membrane-less organelles (MLOs), such as the nucleolus, nuclear paraspeckles, stress granules, and many other ribonucleoprotein granules 1. This functional diversity across numerous MLO subtypes highlights LLPS's ability to fine-tune biochemical reactions by facilitating the rapid assembly and disassembly of organelles and the inclusion or exclusion of specific chemical components 5. Although recent research has revealed that RNAs can modulate protein LLPS behavior 7, our understanding of how cells regulate LLPS per se remains relatively elusive. Uncovering these details has become increasingly urgent following the discovery that dysregulation of LLPS is associated with disease 8. Specifically, prolonged LLPS of proteins such as fused in sarcoma (FUS) 10, heterogeneous nuclear ribonucleoprotein A111, Huntingtin 12, and transactive response DNA-binding protein of 43 kDa (TDP-43) 13 can directly promote protein aggregation into amyloid fibrils, a hallmark of numerous neurodegenerative diseases 4.

Like RNA, DNA also plays a very important role in cells. However, there are few reports on the LLPS of DNA in recent literature. Mechanistically, DNA condensation can be driven by macromolecular crowding, multivalent cations, or positively charged proteins. At low DNA concentrations, condensation triggers the conformational change of individual DNA molecules into a compacted state, with distinct morphologies. Above a critical DNA concentration, condensation goes along with phase separation into a DNA-dilute and a DNA-dense phase. The latter DNA-dense phase can have different material properties and has been reported to be rather liquid-like or solid-like depending on the

characteristics of the DNA and the solvent composition16. Such as droplets. LLPS of biomolecules has garnered considerable attention, as the droplets have an important role in regulating various biological functions7. Several in vitro studies have reproduced droplet formation by changing the concentrations of proteins/RNAs and salts17. For such the LLPS, by measuring the water content of droplets under different conditions, the researchers found that the salt content and stoichiometry of the mixed polyelectrolytes have a significant effect on the droplet composition.

In this paper, we compared the phase diagrams of liquid-liquid phase separation of DNA under different forces and determined that the LLPS was mainly affected by electrostatic interaction.

we use PLL to induce salmon sperm DNA to form LLPS and two kinds of precipitates. In addition, we added ethanol, 6-A and 1,6-hexanediol to the solution respectively, and made a detailed comparison of the formation range of the three products. (1,6-hexanediol is an aliphatic alcohol that is known to disrupt weak protein-protein hydrophobic interactions21. It has been used extensively to modify phase separation induced by hydrophobic interactions. Adding ethanol to the solution, the dielectric constant of the solution is reduced, thus the electrostatic interaction of the final solution will increase. If add 6-A to the solution, the dielectric constant of the solution is increased, the electrostatic interaction of the final solution will reduce23). We determined that the LLPS of DNA is mainly driven by electrostatic interaction, and we made use of the promoting effect of ethanol on the electrostatic attraction of PLL-DNA, delayed the emergence of LLPS, and the inhibitory effect of 6-A on the electrostatic attraction of PLL-DNA, which advanced the emergence of LLPS. Comparing with the previous regulation of LLPS by salt ions and the common regulation of LLPS by various forces, we have realized the adjustment of LLPS formation only by electrostatic interaction, which provides a simpler model for the research of LLPS in the field of DNA. Moreover, we use the solution turbidity curve to further show that LLPS is controllable by electrostatic interaction.

2. Materials and Methods

2.1 Materials

Salmon sperm DNA was purchased from Thermo Fisher Scientific US. Poly-L-lysine was purchased from the Cool Chemistry Conference. Purified water was obtained from the Milli-Q system (Millipore, Billerica, Massachusetts, USA). Tris-hydroxymethyl-aminomethane (Tris), 6-Aminocaproic acid and 1,6-hexanediol were purchased from Sigma-Aldrich. Ethanol was purchased from Macklin Company. All drugs were prepared with 10 mM Tris buffer（PH=7.4）. We repeat all measurements at least 3 times to obtain consistent results, and the standard deviation was calculated accordingly.

2.2 Electrophoretic-mobility measurements

Electrophoretic mobility (EM, μ) was measured using Malvern Zetasizer Nano ZS90 Dynamic light scattering (DLS) equipment with patented M3-PALS technology. The laser source is a He-Ne gas laser (λ = 633 nm) and the light scattering by the avalanche photodiode mounted on the goniometer arm at the direction of the incident radiation. DNA was diluted to a concentration of 1 ng/μl in a Tris buffer in DLS measurement, by adding various agents with a different concentration in solution. Before measurement, 5 min are needed for incubation at room temperature. In the measurement of EM, a sample of 1 mL of DNA solution was pipetted in the folded capillary cell. During the process of measurement, sample cell was kept at a constant temperature of 25 ± 2℃. The measurement has 30 runs each time. We repeat all measurements at least 3 times.

2.3 Microscope imaging

The imaging of LLPS was performed on a Nikon Ti-E inverted microscope equipped with a Nikon 100x oil-immersion objective (Nikon CFI Apo 100XW NIR), a 48MP FHD Camera V8 and Instec MK2000B temperature controller. The Instec MK2000B temperature controller is connected to industrial chiller c100W and semiconductor platform. Before imaging the solution, put the solution into the H1650-W centrifuge for centrifugation, set the 12000 r/min or 1000 r/min and the time to 2 min. Adjust the required temperature, prepare an amicroscope cover glass, took the supernatant and place it on the platform and drop a 30-50 μg/μl DNA solution by adding different concentration of agents. while observing the sample, the imaging time should not be too long to prevent the droplets change.

2.4 UV–vis spectrophotometer

A UV-vis spectrum was measured on a the Q5000 Ultra-micro ultraviolet spectrophotometer (Quawell, USA). 2 μl of the prepared DNA solution by adding different concentration of agents were loaded onto the pedestal of UV-vis spectrophotometer for turbidity measurement at 280 nm. The turbidity (T) is defined by T = -ln(I/I0), with I0 = incident light intensity and I= intensity of light passed through the sample volume. Turbidity is measured in adsorption units (a.u.)25.

2.5 AFM Imaging

We imaged all samples on a commercial Nano Wizard III AFM (JPK Instruments AG, Berlin, Germany) with a liquid box. The sample and cantilever settled for at least 15 min before imaging. The instrument is set to tapping mode, a typical setpoint amplitude of ~2 nm and a free amplitude of 150% of the set point. When the needle goes down into the liquid, the adjustment of the laser is completed. We chose the drive frequency as the closest peak of the drive transfer function to the thermal resonance. Chosing the images of 512 × 512 pixels and a 1 Hz scan rate. The standard 5 × 5 μm2 images were obtained using a Bruker SNL-10A cantilever (r_{nom}≈2 nm; k_{typ} = 350 pN/nm) with a 13 kHz resonance in liquid.

We deposited the sample on the mica for 10 min. Then, rinse with the buffer, and finally keep the 1 mL solution in the liquid box. Each sample is repeated at least three times and is imaged in at least three different parts. The average size of droplets in samples for measured by software to ensure the reliability of the data.

3. Result

3.1 Detection of complex condensation of PLL-DNA

The mixture of opposite charged DNA and PLL in aqueous solution will form complex condensation. Under fully or partially neutralized PLL and DNA are mixed for different charge ratios, the complex condensation could form a dense polymer-rich phase (coacervate phase) and a very dilute polymer deficient phase (aqueous phase), and exist in equilibrium. These can be observed as large unshaped two kinds of complexes (precipitates) or as droplets (LLPS). In addition, we observed that ethanol can promote the conversion of P2 into LLPS. The 6-A could promote the conversion of P1 into LLPS. In earlier work, some researchers have shown that LLPS is inseparable from hydrophobic interaction and electrostatic interaction26. Therefore, we speculate that the influence of the two regulators on the LLPS of PLL-DNA may be due to the change of hydrophobic or electrostatic interaction. Optical micrographs of each type of complex condensation (precipitates, droplets) formed in this study are depicted in Fig. 1.

3.2 Detection of Electrostatic interaction

In a high-concentration multivalent solution of PLL-DNA, the main reason for the change of PLL-DNA solution caused by the two regulators can be predicted by reversing the motion of DNA in the solution by external electric field. EM of DNA, μ, reflecting the net charge of DNA and the counterions condensed at its surface, can be measured by DLS in solution.

The measured electrokinetic properties of PLL-DNA are shown in Fig. 2, in which the EM of condensed DNA is plotted versus the concentrations of PLL. With the concentration of PLL increasing, the PLL could induce DNA to charge neutralization and charge inversion. Charge neutralization or charge inversion usually accompany with conformal change of DNA induced by counterions. And, in this process, it may lead to the formation of LLPS of DNA. However, ethanol can promote the charge neutralization of PLL-DNA and complete the charge inversion in advance at lower PLL concentrations. This means that the electrostatic attraction of PLL-DNA is enhanced by ethanol. In addition, 6-A can inhibit the charge inversion of PLL-DNA, thus reducing the electrostatic attraction of PLL-DNA. It is worth pointing out, after adding 1,6 hexanediol to solution of PLL-DNA, consistent with observations for PLL-DNA images. The results show that the solution change of PLL-DNA is not caused by hydrophobic interaction, but closely related to electrostatic interaction.

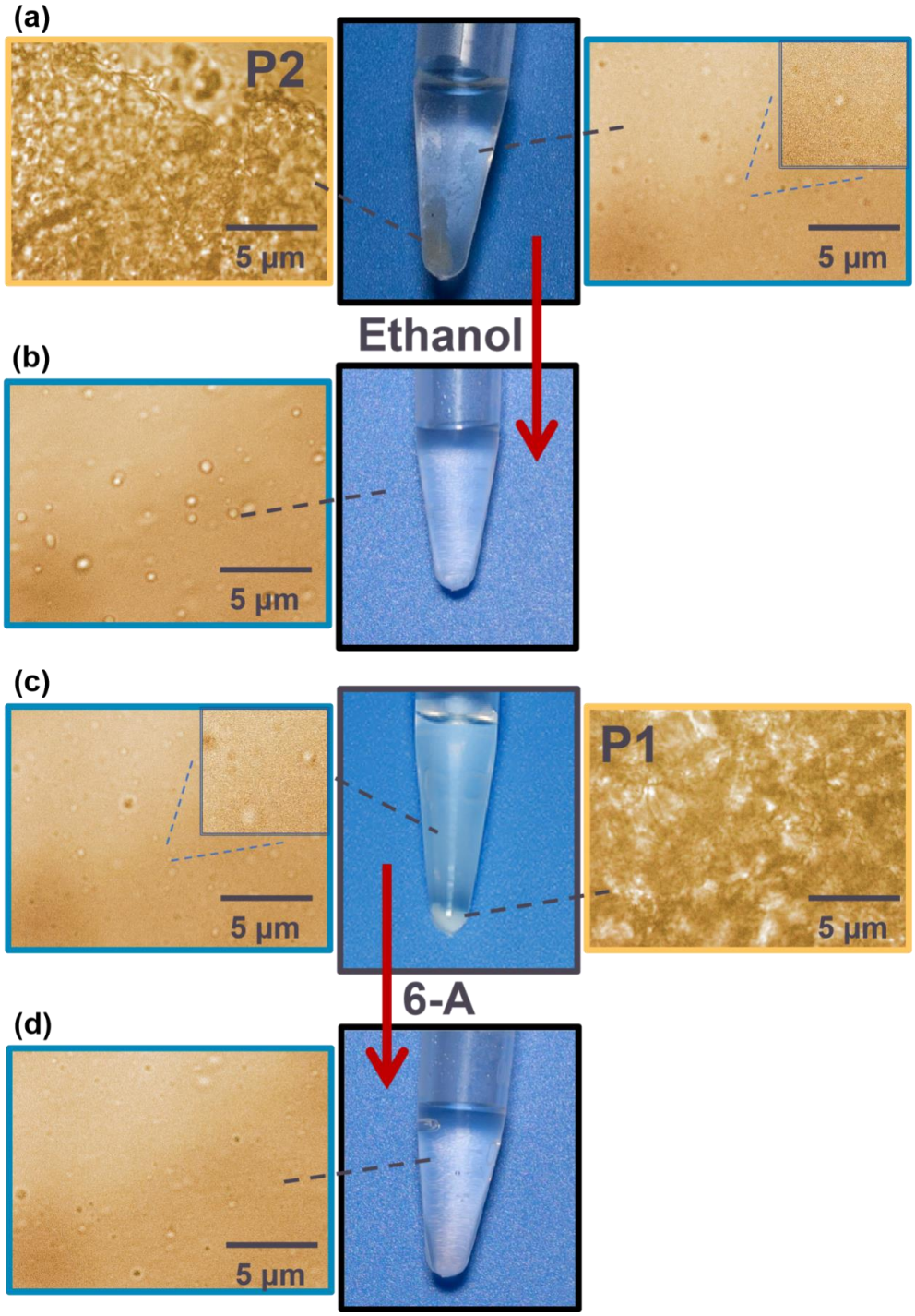

Figure 1. PLL induces complex condensation of the DNA. a: Solution of PLL-DNA with 12000 r/min centrifugal rates in the macroscopic state, PLL=6 μg/μl, DNA= 4 μg/μl. The precipitation 2 (P2) is slightly yellow and sticks to the wall of the centrifuge tube. b: The formation of P2 can be suppressed in the centrifugal tube after adding ethanol 20%. c: Solution of PLL-DNA with 12000 r/min centrifugal rates in the macroscopic state, PLL=6 μg/μl, DNA= 2 μg/μl. The precipitation 1 (P1) is white and packs at the bottom of the centrifuge tube. d: The formation of P1 can be suppressed in the centrifugal tube after adding 6-A 700 mM. In the microscope, we can observe the existence of droplets from the supernatant liquid.

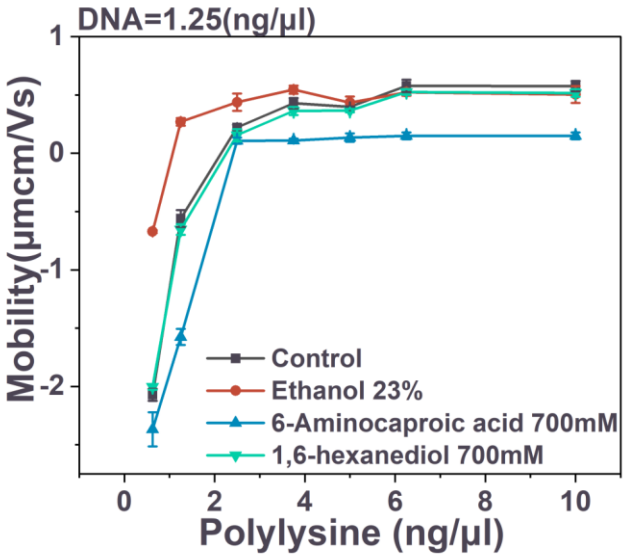

Figure 2. Electrophoretic mobility Analysis of LLPS of DNA. The change diagram of the electrophoretic mobility curve of three regulators and control curve. At the DNA= 1 μg/μl, the curve varies with the concentration of PLL. The curve for 6-A is shown in blue color, ethanol is a red color and 1,6 hexanediol is a green color.

3.3 Detection of LLPS of PLL-DNA in different electrostatic interaction

In order to study the effect of electrostatic interaction on LLPS of PLL-DNA, we drew a phase diagram of PLL-DNA. The critical PLL concentrations required to reach the LLPS boundaries are experimental determined for PLL-DNA and studied the phase change characteristics in different electrostatic interaction. Characteristic phase diagrams of PLL-DNA, formed from DNA with various PLL concentrations, are depicted in Fig. 3.

As seen in Fig. 3a, LLPS is formed after complete neutralization of PLL and DNA (The negative / positive charge ratio (N /P) of PLL-DNA was estimated to be 1). At the DNA= 1 μg/μl, the critical PLL concentrations required for LLPS to reach the range from 0.4 μg/μl to 2 μg/μl in Fig.3e. With the addition of 1,6-hexanediol, there is no marked change in the boundaries of LLPS, are depicted in Fig. 3b, h. Therefore, this once again verifies that hydrophobic interaction does not play a leading role in the LLPS of PLL-DNA.

Notably, after adding the ethanol to solution, the critical PLL concentrations required to reach the LLPS boundaries both are increased in Fig.3c (The N / P of forming LLPS is also increased.). At the DNA= 1 μg/μl, the critical PLL concentrations required for LLPS to reach the range from 0.5 μg/μl to 4.5 μg/μl in Fig.3f. With the addition of 6-A to solution, the critical PLL concentrations required to reach the LLPS boundaries both are reduced in Fig.3d. At the DNA= 1 μg/μl, the critical PLL concentrations required for LLPS to reach the range from 0.35 μg/μl to 1 μg/μl in Fig.3g (The N / P of forming LLPS is reduced.). The result showed that the ethanol increases the electrostatic attraction of PLL and DNA, and more PLL needs to be consumed to form LLPS when the number of DNA is constant. The addition of 6-A weakens the electrostatic attraction of PLL and DNA. When the quantity of DNA is constant, PLL-DNA needs to consume less PLL to form LLPS.

The phase diagram for LLPS is shown in blue color, P1 is a red region and P2 is a yellow region. The color overlap is the coexistence of LLPS and precipitation.

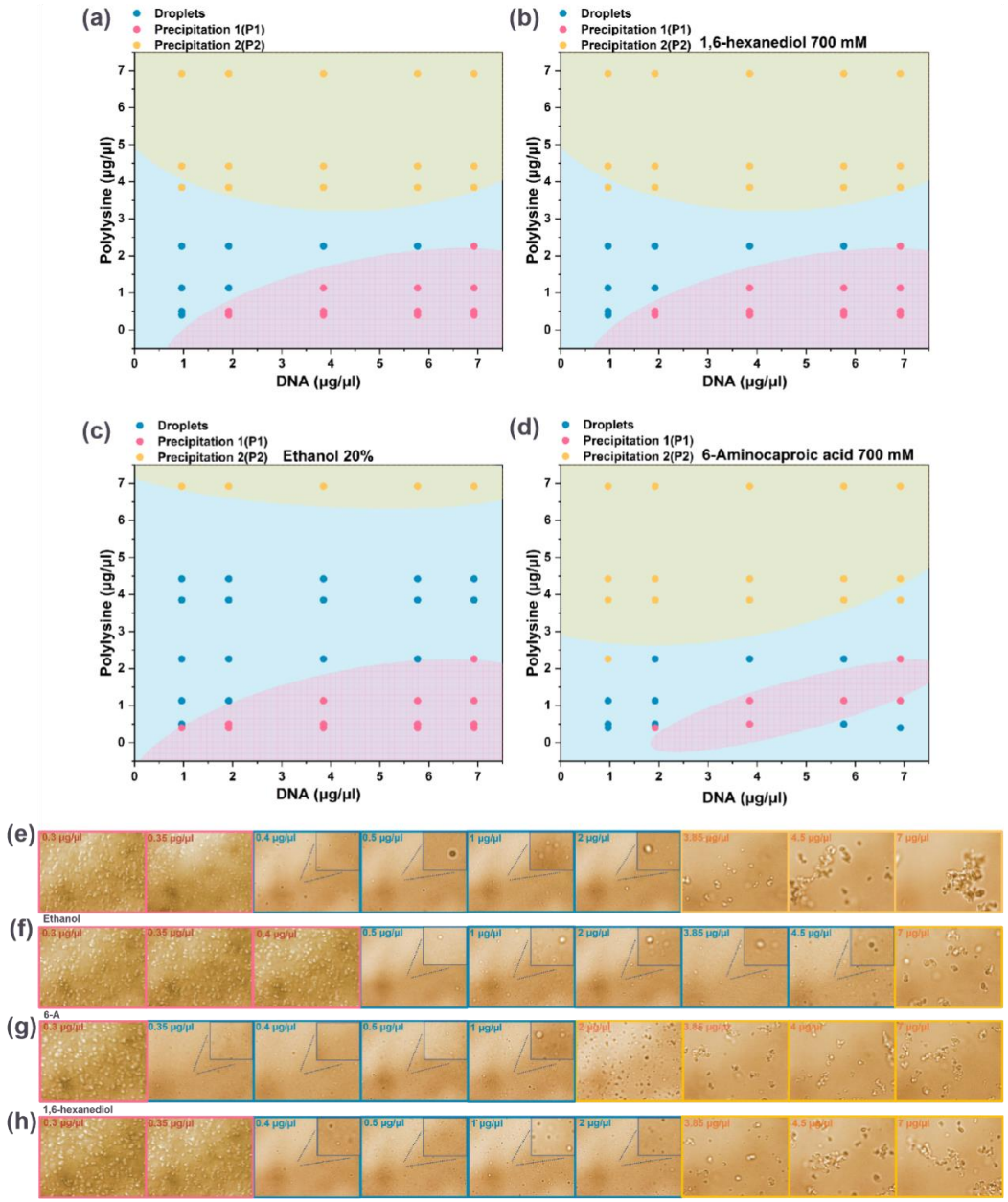

Figure 3. Impact of regulators on LLPS of DNA. a: At 12000 r/min centrifugal rate, the phase diagram of PLL-DNA. b: At 12000 r/min centrifugal rate, adding the 1,6-hexanediol 700 mM to the solution of PLL-DNA. c: At 12000 r/min centrifugal rate, adding the ethanol 20% to the solution of PLL-DNA. d: At 12000 r/min centrifugal rate, adding the 6-A 700 mM to the solution of PLL-DNA. e: At 1000 r/min centrifugal rate and DNA= 1 μg/μl, these can be observed the microscope images of PLL-DNA. f: At 1000 r/min centrifugal rate and DNA= 1 μg/μl, these can be observed the microscope images of PLL-DNA after adding ethanol 20%. g: At 1000 r/min centrifugal rate and DNA= 1 μg/μl, these can be observed the microscope images of PLL-DNA after adding 6-A 700 mM. h: At 1000 r/min centrifugal rate and DNA= 1 μg/μl, these can be observed the microscope images of PLL-DNA after adding 1,6-hexanediol 700 mM.

3.4 The analysis of ultraviolet spectrophotometer for LLPS of PLL-DNA

In order to further understand the specific role of electrostatic interaction in LLPS of PLL-DNA. We use ultraviolet spectrophotometer to detect the light transmission of supernatant liquid of DNA= 1 μg/μl in diffident concentration of PLL (Fig.2a, b). The measured light transmission depends on the size and composition of the droplets formed, thus turbidity can further reflection the extent of LLPS formation.

In aqueous solution, at the DNA= 1 μg/μl, the peak of PLL concentrations required for LLPS is about 2 μg/μl in Fig.4a. With adding 6-A to aqueous solution of PLL-DNA (1 μg/μl), the peak of PLL concentrations required for LLPS is about 0.5 μg/μl in Fig.4b. This means that the N / P of forming LLPS is reduced about from 1 to 0.25. With adding the 1,6-hexanediol to aqueous solution of PLL-DNA (1 μg/μl), the turbidity has little influence in Fig.4c. In addition, with adding ethanol to aqueous solution of PLL-DNA (1 μg/μl), the peak of PLL concentrations required for LLPS is about 4 μg/μl in Fig.4d, which means that the N / P of forming LLPS is increased about from 1 to 2. These results are consistent with our above conclusions. Moreover, we have proved that the change of electrostatic interaction can be used to regulate the formation of LLPS in solution accurately.

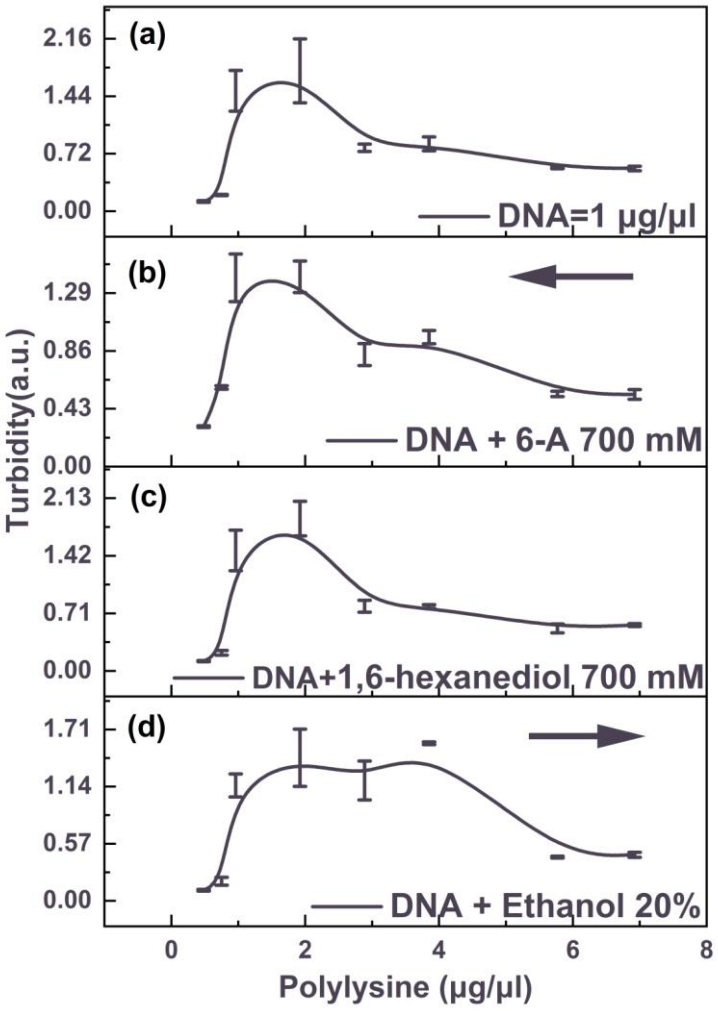

Figure 4. The turbidity of LLPS in PLL-DNA a: The UV-vis turbidity Spectra without regulators addition. b: The comparison of UV-vis turbidity Spectra with adding the 6-A. c: The comparison of UV-vis turbidity Spectra with adding the ethanol. d: The comparison of UV-vis turbidity Spectra with adding the 1,6-hexanediol. At 12000 r/min centrifugal rate, the concentration of PLL from 0.5 μg/μl to 7 μg/μl, DNA=1 μg/μl, 6-A=700 mM, Alcohol=23%, 1,6-hexanediol=700 mM.

3.5 Detection AFM of PLL-DNA in different electrostatic interaction

AFM has been known to be a powerful tool for determining some subtle changes in LLPS conformation. We can infer the binding strength of the PLL and DNA from the change of the morphology of the P1. Thus, the above conjecture is verified and the size of the polymers is further adjusted.

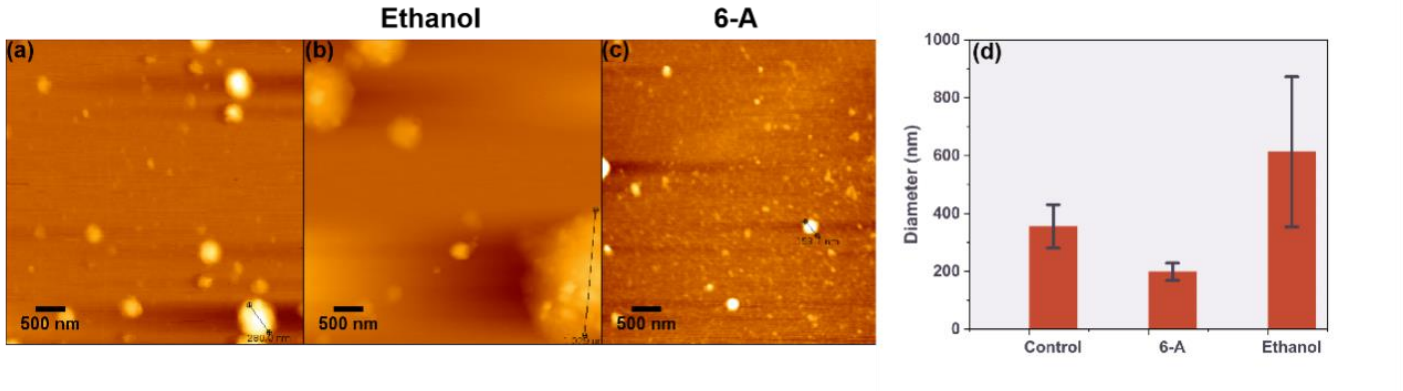

Figure 5. AFM images of polymers in medicine. a: PLL=50 ng/μl, DNA=50 ng/μl (The N/P less than 1). b: PLL=50 ng/μl, DNA=50 ng/μl, Alcohol=23%. c: PLL=50 ng/μl, DNA=50 ng/μl, 6-A=150 mM. d: Statistical diagrams of P1 sizes under different regulator.

According to the Fig. 5a, under the N / P is less than 1, only part of the DNA is neutralized to form P1 by PLL, the PLL-DNA gathered in a round shape in the solution. We made statistics on the average diameter of P1 in the sample, the average of diameter is 400 nm in Fig. 5d. According to Fig. 5b, d, after adding ethanol to solution, the average diameter of the P1 is 600 nm. This shows that the same quentity of DNA can bind more PLL. In addition, after adding 6-A to solution of the PLL-DNA, the diameter of P1 reduced obviously from 400 nm to 200 nm in Fig. 5c, d. This shows that the same quentity of DNA can bind less PLL. Moreover, our interpretation of PLL-DNA 's LLPS is verified.

4. Discussion and Conclusion

Although many recent studies have explored the role of protein sequence and structure in LLPS, there are relatively few studies focused on such aspects of DNA28. Typically, LLPS of biomolecules (droplet formation) is induced via a hydrophobic30 and/or an electrostatic interaction31. In this article, we have realized the use of electrostatic interaction to adjust LLPS.

One possible mechanism has been suggested: a strong correlation effect. This binding is expected to depend on the properties of the ions such as their size, chemical composition, surface structure, and valence32. The strong correlation effect is driven predominantly by electrostatic interactions. In this mechanism, LLPS of DNA is a purely electrostatic phenomenon driven by the existence of a strongly correlated liquid of counterions at the DNA surface and predicted to take place if its effective charge is close to zero34. According to the Fig. 6. With adding the positive PLL, the PLL molecules bind to DNA via arrange along the DNA strands36, when the N / P is less than 1, the P1 is formed. With the concentration of PLL increasing, leading to the surface charge of DNA is neutralized (N / P = 1), thus forming LLPS. When the PLL overcompensate the DNA charge at high PLL concentration (N / P is more than 1), in turn destabilizing the LLPS, the P2 is formed. The addition of ethanol to the solution decreased the dielectric constant, and the water molecules around DNA were preferentially combined with ethanol, thus, DNA has more surface area to combine with PLL and more PLL needs to be consumed to form LLPS. In addition, 6-A can increase the dielectric constant of solution. So, it can inhibit the combination of PLL and DNA, causing DNA only needs to consume a small amount of PLL to fill the opposite charge on the surface.

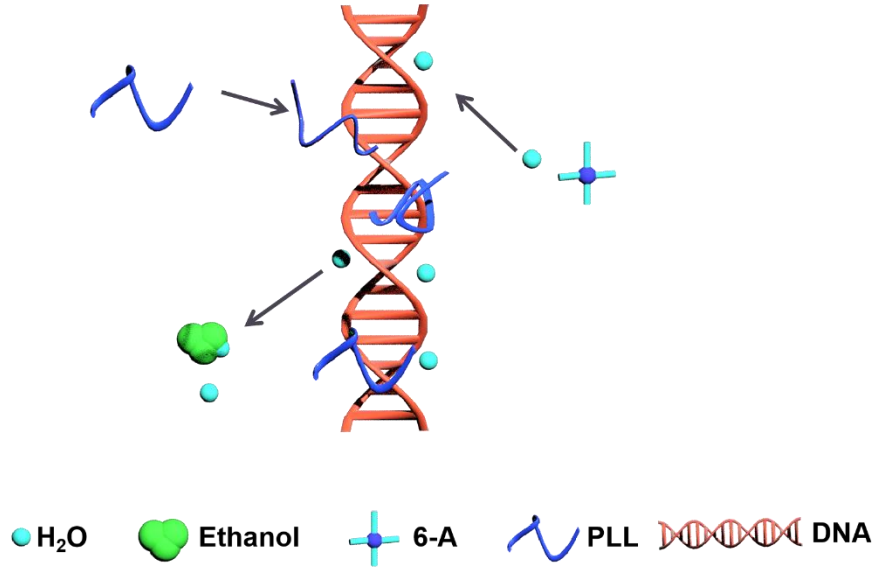

Figure 6. The hypothetic model of the PLL-DNA condensing mechanism through electrostatic interactions.

Acknowledgements

This work is supported by the National Natural Science Foundation of China (12074289, 11574232) and the Natural Science Foundation of Zhejiang Province(LY23A40002). Wenzhou science and Technology Prpject（L20240004）.The 14th Five-Year Plan Teaching Reform Project of Higher Education in Zhejiang Province (JG20220509) and the Graduate Teaching Reform Project (2023-016);Industry-University-Research Project of Ministry of Education(202101003050,202101044006).

References

1. Shin, Y. and C.P. Brangwynne, Liquid phase condensation in cell physiology and disease. Science, 2017. 357(6357): p. eaaf4382.
2. Banani, S.F., et al., Biomolecular condensates: organizers of cellular biochemistry. Nature reviews Molecular cell biology, 2017. 18(5): p. 285-298.
3. Van Treeck, B. and R. Parker, Emerging roles for intermolecular RNA-RNA interactions in RNP assemblies. Cell, 2018. 174(4): p. 791-802.
4. Babinchak, W.M., et al., Small molecules as potent biphasic modulators of protein liquid-liquid phase separation. Nature communications, 2020. 11(1): p. 1-15.
5. Pancsa, R., et al., Emergent functions of proteins in non-stoichiometric supramolecular assemblies. Biochimica et Biophysica Acta (BBA)-Proteins and Proteomics, 2019. 1867(10): p. 970-979.
6. Dolgin, E., The shape-shifting blobs that shook up cell biology. Nature, 2022. 611: p. 24-27.
7. Maharana, S., et al., RNA buffers the phase separation behavior of prion-like RNA binding proteins. Science, 2018. 360(6391): p. 918-921.
8. Nedelsky, N.B. and J.P. Taylor, Bridging biophysics and neurology: aberrant phase transitions in neurodegenerative disease. Nature Reviews Neurology, 2019. 15(5): p. 272-286.
9. Ryan, V.H. and N.L. Fawzi, Physiological, pathological, and targetable membraneless organelles in neurons. Trends in neurosciences, 2019. 42(10): p. 693-708.
10. Patel, A., et al., A liquid-to-solid phase transition of the ALS protein FUS accelerated by disease mutation. Cell, 2015. 162(5): p. 1066-1077.
11. Molliex, A., et al., Phase separation by low complexity domains promotes stress granule assembly and drives pathological fibrillization. Cell, 2015. 163(1): p. 123-133.

12. Peskett, T.R., et al., A liquid to solid phase transition underlying pathological huntingtin exon1 aggregation. Molecular cell, 2018. 70(4): p. 588-601. e6.
13. Babinchak, W.M., et al., The role of liquid–liquid phase separation in aggregation of the TDP-43 low-complexity domain. Journal of Biological Chemistry, 2019. 294(16): p. 6306-6317.
14. Chiti, F. and C.M. Dobson, Protein misfolding, amyloid formation, and human disease: a summary of progress over the last decade. Annu. Rev. Biochem, 2017. 86(1): p. 27-68.
15. Kulakowski, B.T., J.F. Gardner, and J.L. Shearer, Dynamic modeling and control of engineering systems. 2007: Cambridge University Press.
16. Muzzopappa, F., M. Hertzog, and F. Erdel, DNA length tunes the fluidity of DNA-based condensates. Biophysical Journal, 2021. 120: p. 1288 - 1300.
17. Elbaum-Garfinkle, S., et al., The disordered P granule protein LAF-1 drives phase separation into droplets with tunable viscosity and dynamics. Proceedings of the National Academy of Sciences, 2015. 112: p. 7189 - 7194.
18. Franzmann, T.M., et al., Phase separation of a yeast prion protein promotes cellular fitness. Science, 2018. 359.
19. Berry, J., et al., RNA transcription modulates phase transition-driven nuclear body assembly. Proc Natl Acad Sci U S A, 2015. 112(38): p. E5237-45.
20. Quesada-Pérez, M., et al., Overcharging in colloids: beyond the Poisson-Boltzmann approach. Chemphyschem, 2003. 4(3): p. 234-48.
21. Itoh, Y., et al., 1,6-hexanediol rapidly immobilizes and condenses chromatin in living human cells. Life Sci Alliance, 2021. 4(4).
22. Düster, R., et al., 1,6-Hexanediol, commonly used to dissolve liquid-liquid phase separated condensates, directly impairs kinase and phosphatase activities. J Biol Chem, 2021. 296: p. 100260.
23. Wang, Y., et al., Single Molecular Demonstration of Modulating Charge Inversion of DNA. Sci Rep, 2016. 6: p. 38628.
24. Fedorchuk, T.P., et al., One-Pot Biocatalytic Transformation of Adipic Acid to 6-Aminocaproic Acid and 1,6-Hexamethylenediamine Using Carboxylic Acid Reductases and Transaminases. J Am Chem Soc, 2020. 142(2): p. 1038-1048.
25. Priftis, D. and M. Tirrell, Phase behaviour and complex coacervation of aqueous polypeptide solutions. Soft Matter, 2012. 8(36): p. 9396-9405.
26. Krainer, G., et al., Reentrant liquid condensate phase of proteins is stabilized by hydrophobic and non-ionic interactions. Nature communications, 2021. 12(1): p. 1-14.
27. Wang, J., et al., A molecular grammar governing the driving forces for phase separation of prion-like RNA binding proteins. Cell, 2018. 174(3): p. 688-699. e16.
28. Weber, S.C., Sequence-encoded material properties dictate the structure and function of nuclear bodies. Current opinion in cell biology, 2017. 46: p. 62-71.
29. Shakya, A. and J.T. King, DNA Local-Flexibility-Dependent Assembly of Phase-Separated Liquid Droplets. Biophysical Journal, 2018. 115: p. 1840 - 1847.
30. Chong, S., et al., Imaging dynamic and selective low-complexity domain interactions that control gene transcription. Science, 2018. 361.
31. Nott, T.J., et al., Phase Transition of a Disordered Nuage Protein Generates Environmentally Responsive Membraneless Organelles. Molecular Cell, 2015. 57: p. 936 - 947.
32. Quesada-Pérez, M., et al., Overcharging in colloids: beyond the Poisson–Boltzmann approach. 2003. 4(3): p. 234-248.
33. Shklovskii, B.I.J.P.R.E., Screening of a macroion by multivalent ions: correlation-induced inversion of charge. 1999. 60(5): p. 5802.
34. Rouzina, I. and V.A. Bloomfield, Macroion attraction due to electrostatic correlation between screening counterions. 1. Mobile surface-adsorbed ions and diffuse ion cloud. The Journal of Physical Chemistry, 1996. 100(23): p. 9977-9989.
35. Shklovskii, B.I., Wigner crystal model of counterion induced bundle formation of rodlike polyelectrolytes. Physical review letters, 1999. 82(16): p. 3268.
36. Li, G.-Y., et al., DNA condensation induced by metal complexes. Coordination Chemistry Reviews, 2014. 281: p. 100-113.